Available online at www.sciencedirect.com
SCIENCE DIRECT
International Journal of Heat and Mass Transfer 49 (2006) 3417–3428
International Journal of HEAT and MASS TRANSFER
www.elsevier.com/locate/ijhmt

Gas entrainment in an evaporating spray jet

Muhammad Mushahid Rafique Qureshi, Chao Zhu *

Department of Mechanical Engineering, New Jersey Institute of Technology, Newark, NJ 07102, USA

Received 14 August 2005; received in revised form 11 March 2006
Available online 22 May 2006

Abstract

Gas entrainment induced by a spray jet can be significantly affected by the spray evaporation rate. In this study, we have directly measured the air entrainment induced by a liquid nitrogen spray jet into an unbounded and stagnant room air. It is realized that the air entrainment is proportional to the axial gradient of oxygen mass flow in a pure nitrogen spray jet. Hence, the air entrainment can be determined by a combined measurement of local cross-sectional distributions of oxygen concentration, gas temperature and gas velocity along the jet path. These measurements are directly obtained using an in situ oxygen concentration analyzer, a thermocouple system, and a Laser Doppler Velocimeter. In order to evaluate the effect of evaporation rate, direct measurements and numerical simulations of the air entrainment by a cold gaseous jet of nitrogen (at a temperature slightly above that of liquid nitrogen) into room air are also performed. Measurements of the entrainment rate and flow similarity of the gaseous jets without droplets compared very well against those from the single-phase jet theories and numerical simulation, which validates our experimental approach and analysis method. Our experimental results indicate rough flow similarities exist in evaporating spray jets with round nozzles. Although the air entrainment by the liquid nitrogen spray is found significantly increased, as compared to that by the cold gaseous jet of nitrogen from the same nozzle and at the same jetting velocity, the increased ratio is far less than the equivalent momentum ratio of the liquid nitrogen spray to the gas nitrogen jet. This experimental finding suggests that the evaporation of spray markedly weakens the gas entrainment. In this study, a parametric model is also developed to provide a theoretical basis of the data analysis for the cross-section averaged spray evaporation rate within the spray jet region.

Keywords: Evaporating spray jets; Entrainment rate; Evaporation rate

1. Introduction

Evaporating spray jets are used in many industrial applications such as feed oil sprays in the petroleum refinery, spray drying, liquid fuel sprays in engine combustion, and spray-assisted coal gasification. Spray with a rapid evaporation can have a strong influence on the jet entrainment that in turn affects the evaporation rate and hence spray penetration. Hence, it is interesting to investigate the interacting effects of the spray jet entrainment and the spray evaporation rate.

The entrainment characteristics and flow similarity of single-phase jets have been extensively studied [1]. For non-conventional single-phase jets such as a plunging jet to a liquid surface and plasma jets, the air entrainment, temperature and velocity similarities have also been investigated [2–4]. For two-phase non-evaporating swirling jets, the entrainment is greatly suppressed for a two-phase jet as compared to single-phase jets [5]. For a cross-flow spray jet without evaporation, the ratio of the cross-wind speed to the induced air speed governs the movements of the spray droplets. The flow at a high ratio may even diminish the entrainment [6]. The entrainment rates of reacting/non-reacting jets were compared using the mass balance technique as well as by a velocity field measurement using particle image velocimeter (PIV) [7]. However, neither temperature nor concentration measurements were reported in their study. Studies on the entrainment of two-phase (gas–solid) surrounding media by a gas jet have been reported

* Corresponding author. Tel.: +1 973 642 7624; fax: +1 973 642 4282.
E-mail address: chao.zhu@njit.edu (C. Zhu).

0017-9310/$ - see front matter © 2006 Elsevier Ltd. All rights reserved.
doi:10.1016/j.ijheatmasstransfer.2006.03.006

Nomenclature

A	cross-sectional area, m^2
b	boundary of the jet based on concentration, m
C	concentration of oxygen, %
c_p	specific heat at constant pressure, kJ/kg K
D	diameter of the nozzle, m
E	energy flux, kJ/s
J	mass flux, kg/s
J_{mj}	total jetting mass flow rate, kg/s
J_{dj}	liquid jetting mass flow rate, kg/s
L	specific latent heat, kJ/kg
L_e	evaporation length, m
P	pressure, Pa
R	gas constant, kJ/kg K
r	radial distance from the center of the jet, m
T	temperature, K
U	gas velocity, m/s
z	axial distance from the nozzle exit, m

Greek symbols

ρ	density of the air, kg/m^3
Γ	evaporation rate per unit volume, $kg/s\ m^3$

Subscripts

0	centerline value
∞	ambient condition
e	entrained quantity
O_2	oxygen based quantity
d	cross-section averaged droplet quantity
j	quantity value at the jet exit

Superscript

*	dimensionless quantity

[8–10]. The entrainment velocity is found to decrease with the distance from nozzle, increase with the nozzle velocity and decrease with the solid loadings. Our literature survey shows that there appears no previous study reported on the coupling nature of spray vaporization and spray-jet induced gas entrainment.

This paper aims to address the important subject that has never been studied before: evaporation effect of droplets on gas entrainment of a spray jet. In this study, we have performed an experimental study of a liquid nitrogen spray into the room air. Direct measurements of the oxygen concentration and droplet velocity in the spray region are obtained, based on which the air entrainment and spray evaporation rate are calculated. Due to the difficulties in premixing tracer particles into the liquid nitrogen system and from the direct contact of droplets with thermocouples, the direct measurements of gas velocity and gas temperature in the liquid nitrogen spray region cannot be obtained via LDV and thermocouple measurements. The limited size of spray nozzle also prevents an accurate measurement of radial profile in the near field of the liquid nitrogen spray jet. Alternatively we assume that the dimensionless distribution of gas temperature in the spray region is the same as that of concentration; and the dimensionless gas velocity can be represented by that in the absence of spray. These assumptions have been partially validated from the comparison of direct measurements of oxygen concentration with and without spray, from the numerical simulation of liquid nitrogen spray in a co-axial gas–solid flow [11], and from the comparison of temperature and concentration measurements in the absence of spray.

Besides the measurements, a parametric model has been developed to provide the theoretical basis of data analysis, which is to solve for three coupled unknowns: gas entrainment velocity, spray evaporation rate, and centerline gas velocity. The measurement and modeling methodology, in principle, do not require the use of any similarity laws. However, to simplify the data analysis, as suggested from our measurements and previous numerical simulations [11] within the tolerance range, we used the similarity as an engineering approximation.

2. Experimental approaches

There are two experimental setups in this study. One is for the gas entrainment with a cold nitrogen gas jet, which is to provide a comparison base for the study with spray, and the other is for the gas entrainment with a liquid nitrogen spray. Fig. 1(a) shows a combined schematic diagram of both experimental setups. When valve A is open and valve B is closed, a very cold jet of nitrogen gas (at approximately the temperature of liquid nitrogen) is generated from a compressed nitrogen gas container by passing through a heat exchanger submerged in liquid nitrogen. The cold gas jet is then injected into the stagnant room air. Conversely, if valve A is closed and valve B is open, Fig. 1(a) then represents the schematics of the experimental apparatus for evaporating spray jets, where the sprays of liquid nitrogen are generated from a pressure-controlled spray generation system (25-l, Brymill Cryogenic). This system hence is capable of producing a sustained spray jet of liquid nitrogen. The sustainability depends on the size of nozzle and the operation pressure inside the liquid nitrogen tank. In this study, a sustained liquid nitrogen spray with a constant flow rate is obtained for approximately 40 min. Fig. 1 (b) shows the detailed structure of the spray nozzle, which consists of a small centerline tube (1 mm in

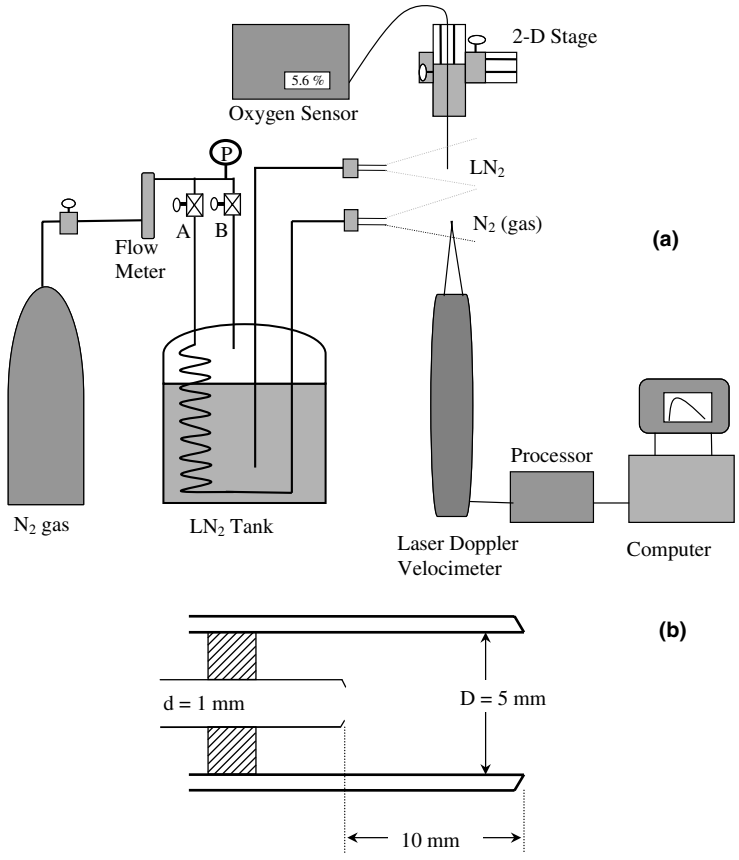

Fig. 1. Experimental setup: (a) schematic for cold nitrogen gas jet (near LN_2 temperature) or for LN_2 spray jet and (b) nozzle structure for a LN_2 spray jet.

diameter) for atomization and a coaxial and thermally-insulated tube (5 mm in diameter) for spray confinement and smoothing. This nozzle structure helps to generate a liquid nitrogen spray with a reasonably large initial spray diameter, which is needed for our measurements of spray radial profiles near the spray nozzle.

An in situ oxygen concentration analyzer (CE0123, Oxigraf) with a thermal compensation and control mechanism is specially designed for measurements of oxygen concentration at extremely low temperatures. The oxygen sensor probe (1.25 mm orifice) is mounted on a precision 3-D stage. This oxygen analyzer is capable of measuring the oxygen concentration with an accuracy of 0.1%, and the measurements are independent of sample pressure, gas temperature and other gases such as CO_2 or H_2O. The temperature profiles are obtained using a tiny Type-J thermocouple (0.5 mm O.D.) connected to a PC-based temperature measurement system. A Laser Doppler Velocimeter (Flowlite 1-D, Dantec) is used for the measurement of spray jetting velocity as well as axial distributions of droplet velocity along the spray jet. The interrogation region in the LDV measurement is an intersection of two laser beams of waist diameter of 1 mm each. A PC-based precision balance (SV-30, Acculab) is employed to measure the mass flow rate of the spray injection. For nitrogen gas jet, the jetting velocity is obtained from the flow rate measurement using a rotary flow meter.

3. Theoretical basis and methodology

Our modeling approach takes the advantages of the fact that, in a free spray jet of liquid nitrogen injected into the air, liquid nitrogen evaporation does not contribute to the amount of oxygen in the spray region, and all oxygen found in the spray region is solely from the jet-induced entrainment. Hence, the air entrainment between any two jet cross-sections is proportional to the difference of oxygen mass flows at these two cross-sections. The proportionality depends on the ambient oxygen concentration. In the room air with the oxygen concentration of 21%, this proportionality is 4.76. In the following we first describe the general equations and methodology of this model, and then we extend our discussion to special applications where jet flow similarities hold. The introduction of flow similarity can greatly reduce both the complicity in equation solution processes and the demand of extensive measurements in the spray region. As shown from measurements in the section of results and discussion, it is reasonable to assume flow similarities in this study.

3.1. Governing equations

Consider an arbitrary jet cross-section segment shown in Fig. 2. The oxygen mass flow rate J_{O_2} across any jet cross-section is given by

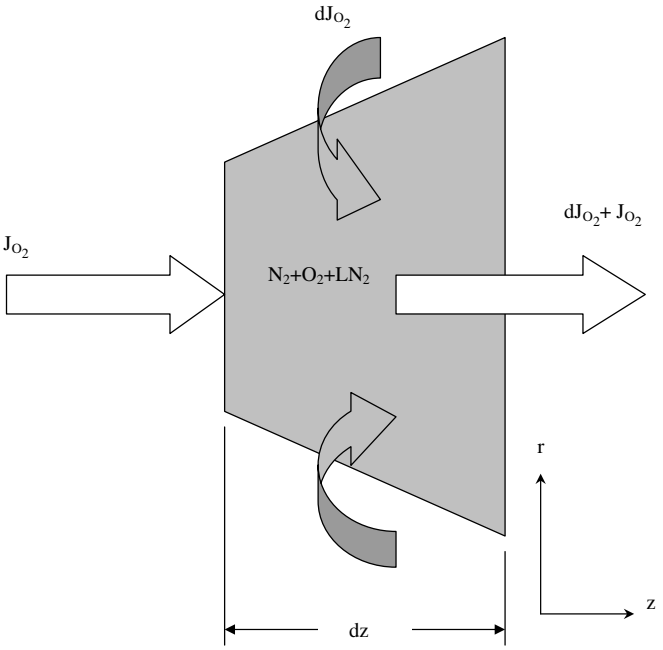

Fig. 2. Gas entrainment (oxygen) from mass flow balance.

$$J_{O_2} = \int_0^\infty 2\pi r \rho C U \, dr \tag{1}$$

where ρ is the overall density of all gaseous species, C is the oxygen concentration, and U is the gas velocity. Assuming that the overall gas follows the ideal gas law and the ambient pressure and the gas constant remain unchanged with the liquid nitrogen evaporation, we have

$$\rho = \frac{P}{RT} \tag{2}$$

where P is the ambient pressure, R is the gas constant and T is the temperature of ambient air.

Hence, the oxygen mass flow rate, which is a function of axial location itself, depends solely on the radial distribution of the velocity, concentration and temperature. From the mass balance of oxygen, the radial component of the air entrainment velocity U_e is thus given by

$$U_e \approx \frac{1}{2\pi b C_\infty \rho_\infty}\left(\frac{dJ_{O_2}}{dz}\right) \tag{3}$$

where z is the distance from the nozzle exit and b is the jet width.

The heat convection of gas phase $\dot{E}$ at any jet cross-section is calculated by

$$\dot{E} = \int_0^\infty 2\pi r \rho U c_p T \, dr \tag{4}$$

where c_p is the specific heat at constant pressure of nitrogen. Thus, assuming infinite-fast heat and mass transfer, the energy balance over a jet spray segment with a thickness of Δz can be expressed by

$$\dot{E} + 2\pi b U_e \rho_\infty c_p T_\infty \Delta z - L\left(\int \dot{\gamma}\, dA\right)\Delta z \approx \dot{E} + \frac{d\dot{E}}{dz}\Delta z \tag{5}$$

where L is the specific latent heat, and $\dot{\gamma}$ is the local mass evaporation rate per unit volume. It is convenient to define the cross-section-averaged rate of mass evaporated of liquid nitrogen per unit volume, Γ, as

$$\Gamma = \frac{1}{A}\int \dot{\gamma}\, dA \tag{5a}$$

so that Eq. (5) is simplified into an equation for the estimation of Γ:

$$\Gamma \approx \frac{1}{L\pi b^2}\left(2\pi b U_e \rho_\infty c_p T_\infty - \frac{d\dot{E}}{dz}\right) \tag{6}$$

Another important physical law is the momentum conservation. For a horizontal spray jet, the total momentum along the jet direction is conserved at any jet cross-section. For simplicity, we neglect the Archimedean effect on the jet deflection and jet asymmetry, as observed and partially validated from our experiments. We further assume that the droplet velocity only varies along the jetting direction. Hence, the jet-directional momentum conservation of this two-phase flow at any jet cross-section is given by

$$J_{mj} U_j = \int_0^\infty 2\pi r \rho U^2 \, dr + J_d U_d \tag{7}$$

where J_{mj} is the total jetting mass flow rate at the nozzle exit; U_j is the jetting velocity at the nozzle exit; U_d is the cross-section averaged droplet velocity; and J_d is the cross-section averaged droplet mass flow rate, which can be linked to the spray evaporation rate per unit volume by

$$J_d \approx J_{dj} - \int_0^z \pi b^2 \Gamma \, dz \tag{8}$$

where J_{dj} is the jetting liquid mass flow rate at the nozzle exit. Based on Eq. (8), the evaporation length L_e can be defined and calculated from the mass balance of liquid nitrogen as

$$J_{dj} \approx \int_0^{L_e} \pi b^2 \Gamma \, dz \tag{9}$$

Based on the three independent governing equations (3), (6) and (7), respectively representing the mass, heat and momentum conservation, three independent variables can be solved. In this study, the distributions of oxygen concentration, droplet velocity, and gas temperature in the spray region can be determined, either from the direct measurements or based on the analogy between temperature and concentration profiles. Thus, in principle, the three unknowns, namely the gas entrainment velocity U_e, spray evaporation rate Γ, and the averaged gas velocity U, can be obtained by solving the coupled governing equations.

3.2. Solution procedures with flow similarity

In jet flow applications, when flow similarities exist, the introduction of flow similarity can significantly simplify the equation solution processes as well as reduce the demand of extensive measurements in spray region. With the flow

similarity, it is convenient to express the governing equations with dimensionless variables. Here, we define

$$r^* = \frac{r}{b}, \quad C^* = \frac{C_\infty - C}{C_\infty - C_0}$$
$$U^* = \frac{U_\infty - U}{U_\infty - U_0}, \quad T^* = \frac{T_\infty - T}{T_\infty - T_0} \tag{10}$$

where b is the jet width, r is the radial distance from the center of the jet, T is the temperature inside the jet and the subscripts of 0 and ∞ denote, respectively, the centerline and ambient locations, and superscript $*$ stands for the dimensionless quantity.

Conceptually, the jet boundaries of velocity, temperature and concentration are different [1]. There exists an analogy between the profiles of temperature and concentration so that the jet widths of temperature profile and concentration profile are about the same whereas the jet width of velocity profile is narrower than those of temperature and concentration profiles [1]. In a spray jet with strong vaporization of droplets, the effect of droplet vaporization minimizes the difference of these jet widths [12]. To simplify our analysis of spray jets with strong vaporization, the jet boundary is assumed to be the same for the gas velocity, temperature and concentration. This assumption is partially validated in our measurements, as shown in Fig. 5.

Substituting Eqs. (2) and (10) into Eq. (1) and noting that, for a free jet, $U_\infty = 0$, we have

$$J_{O_2} \approx 2\pi b^2 \frac{P}{R} U_0 \int \left(\frac{r^* U^* \{C_\infty - (C_\infty - C_0) C^*\}}{T_\infty - (T_\infty - T_0) T^*} \right) \mathrm{d}r^* \tag{11}$$

where P, R, U_0, C_0, C_∞, T_0 or T_∞ is either a constant or a function of axial location (z) only; and the jet boundary b is defined based on the dimensionless radial profiles of concentration. Specifically, the jet widths are measured using the interpolation on the dimensionless concentration profiles using the 5% cut-off criterion. Theoretically, a more stringent criterion of 1% can be applied to better define the jet boundary. However, considering the jet-induced fluctuations and uncertainties in the concentration measurements, the 5% cut-off criterion is preferred and used throughout this study.

Similarly, the heat convection of gas phase $\dot{E}$ at any jet cross-section is expressed, according to Eqs. (4) and (3), by

$$\dot{E} \approx 2\pi b^2 c_p \frac{P}{R} U_0 \int_0^1 r^* U^* \, \mathrm{d}r^* \tag{12}$$

In this study, the jet boundary b and oxygen concentration distributions are directly obtained from the oxygen concentration measurements, which yield both r^* and C^*. Due to the collision of liquid nitrogen droplets with the thermocouple, the gas temperature is difficult to be directly measured in the spray region [13]. The dimensionless profile of gas temperature in the spray region is assumed to be the same as that of oxygen concentration, i.e., $T^* = C^*$. This assumption is based on the analogy of similar concentration and temperature profiles for single-phase gas jets. This analogy has been proved for many single-phase jets [1] as well as for a cold nitrogen jet (at a jetting temperature slightly above the liquid nitrogen temperature) into the room air, based on our direct measurements of oxygen concentration and temperature in the jet region as shown in Fig. 6. In a spray region, the effect of strong evaporation of liquid nitrogen droplets leads to a lowered gas temperature as well as a diluted oxygen concentration simultaneously. Hence, the assumption of similar gas temperature and gas concentration profiles in the presence of strong evaporation is reasonable. This assumption is partially validated by a numerical study of the liquid nitrogen spray jets in concurrent dilute gas–solid flows [12]. The centerline gas temperature in the liquid nitrogen spray is found to be very close to that of liquid nitrogen temperature [12], so that $T_0 \approx T_\mathrm{d}$. The droplet velocity U_d is determined directly from the LDV measurements.

Difficulty also rises to the determination of gas velocity profiles in the spray region. Firstly, the only naturally-available "tracers" in a liquid nitrogen spray are the droplets of liquid nitrogen. It is difficult to add or premix other tracers into the liquid nitrogen spray, due to the extremely-low temperature of liquid nitrogen as well as the limited size of liquid nitrogen nozzle system. Secondly, the dense population of droplets in the near field of spray jet and the poly-atomization in liquid nitrogen droplets make the LDV measurements inapplicable to the determination of gas velocity in the spray region. In addition, the limited size of spray nozzle also prevents an accurate measurement of radial profile in the near field of the liquid nitrogen spray jet. Hence, in this study, we assume that the dimensionless profile of gas velocity in the spray jet is the same as that in the cold gas jet, as partially validated by our previous numerical investigation of liquids nitrogen sprays in gas–solids suspensions [11]. However, the centerline gas velocity is still unknown, which is to be solved along with the gas entrainment velocity and the evaporation rate from the governing equations.

4. Results and discussion

Table 1 lists the parameters of nitrogen gas jets and liquid nitrogen spray jet with a round nozzle in this study. All jets are injected into the stagnant room air. The room air temperature is maintained at 297 K.

4.1. Validation of the experimental system and measurement methods

It is important to validate our experimental approaches on the jet measurements. In order to do that, we have first studied gaseous jets of nitrogen in the stagnant air. Fig. 3 illustrates the concentration profiles at different axial locations. It shows that the centerline concentration oxygen increases while the jet boundary expands along the jet path as more air is entrained. The dimensionless concentrations are plotted against the well-known correlation $C^* = 1 - r^{*3/2}$ [1], as shown in Fig. 4. The "negative" r^* in Fig. 4 only

Table 1
Parameters of gas and spray jets

Jet type	Jet temperature (K)	Nozzle diameter (mm)	Jetting velocity (m/s)	Jetting mass flow rate (g/s)	Jet Reynolds number
Nitrogen gas jet (isothermal)	291	5	30	0.64	10,700
Nitrogen gas jet (non-isothermal)	118	5	26	1.76	49,000
Liquid nitrogen spray	74	5	23	3.64	570,000

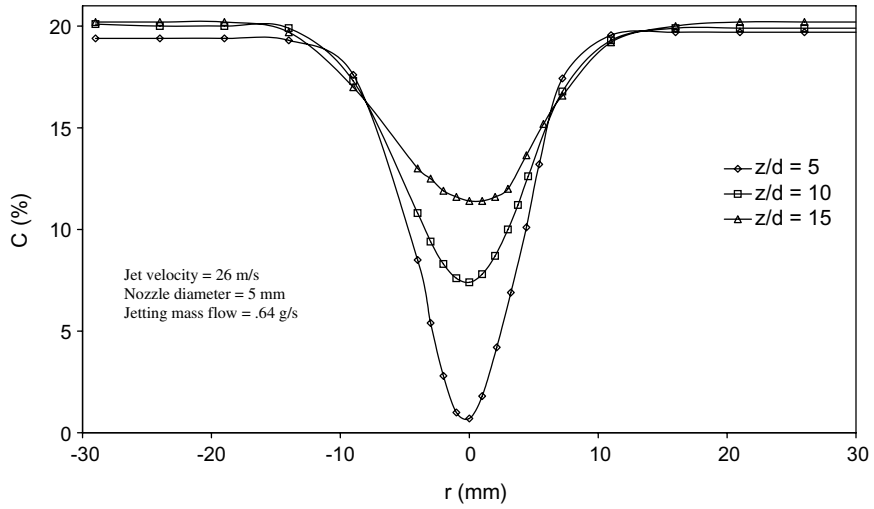

Fig. 3. Oxygen concentration radial profiles in an isothermal nitrogen gas jet.

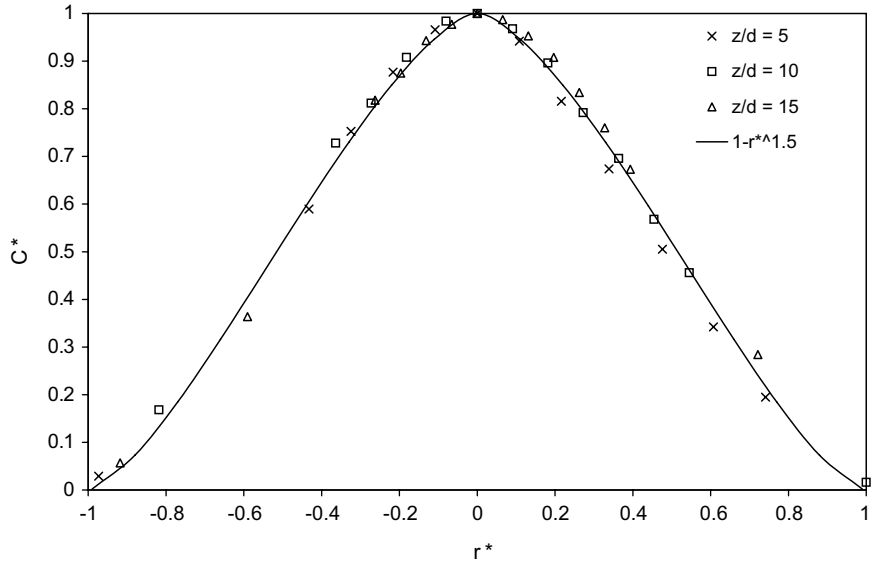

Fig. 4. Dimensionless oxygen concentration radial profiles (with theoretical comparison) in an isothermal nitrogen gas jet.

indicates the measured profile in the opposite side of a complete radial traverse, which is intended to show the symmetric nature of the profile. When a correlation is applied, only positive value of r^* should be used throughout this study. The experimental data matches the above mentioned curve very well. The comparison of measured jet boundary expansion and predictions from Abramovich's jet model [1] $b/z = 0.11(1 + \rho_\infty/\rho_j)$ is shown in Fig. 5. The difference can be caused by several different factors, including the effect of turbulence and the effect of nozzle structure (such as shape of nozzle tip). Another factor is the difference in definition of b. In the Abramovich's model, b is defined with 1% cut-off whereas in this study it is defined from the dimensionless concentration profiles with 5% cut-off. Given the influence of these factors, the experimental data for the boundary expansion of both iso-

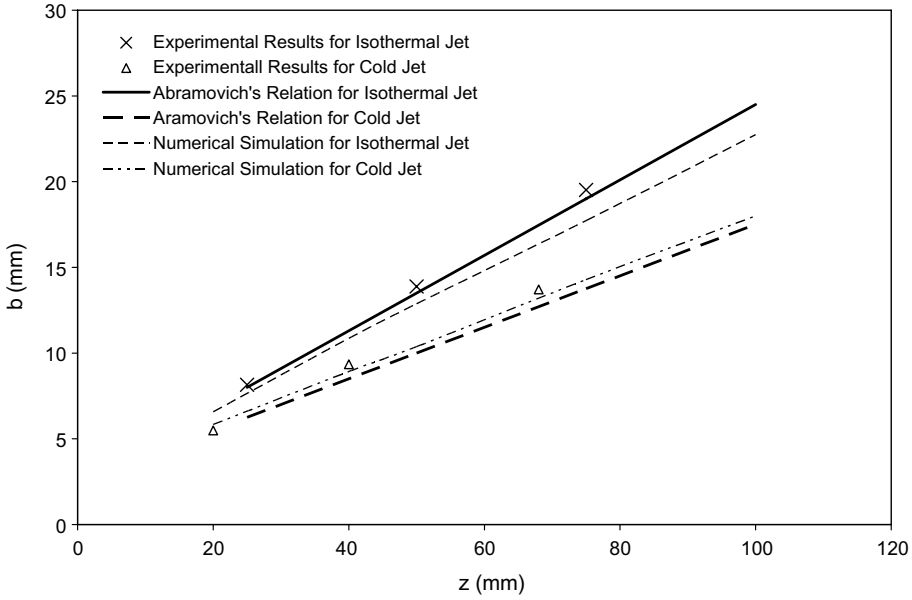

Fig. 5. Jet expansions (with theoretical comparison) of nitrogen gas jets.

thermal and cold nitrogen jets are regarded quite close to the Abramovich's relation. Hence, the comparison between the measurements and well-known correlations in Figs. 4 and 5 validates our experimental system and measurement methods.

4.2. Radial distributions and similarity

According to Eqs. (3) and (6), in order to obtain the air entrainment and spray evaporation rate, one must predetermine the oxygen mass flow, which calls for the information on the radial distributions of oxygen concentration, gas velocity and gas temperature at any spray jet cross-sections. While the oxygen concentration profile can be directly measured using the oxygen probe and analyzer, the direct measurements of local gas temperature and velocity in the presence of fast-moving and evaporating droplets turn out to be extremely difficult, if not impossible, by use of the thermocouple and LDV measurement techniques. The difficulties arise from the interference with the second phase, i.e., the droplet phase. Due to the direct collision of droplets with the thermocouple in the spray region, the measured temperature represents only a mixed temperature of gas and liquids rather than the temperature of gas [13]. In the particle-free spray region where there are no tracing particles representing the gas phase, LDV measures only the velocities of droplets but not the velocity of the gas. Hence, an alternative means for determining the radial distributions of gas temperature and velocity is adapted in this study.

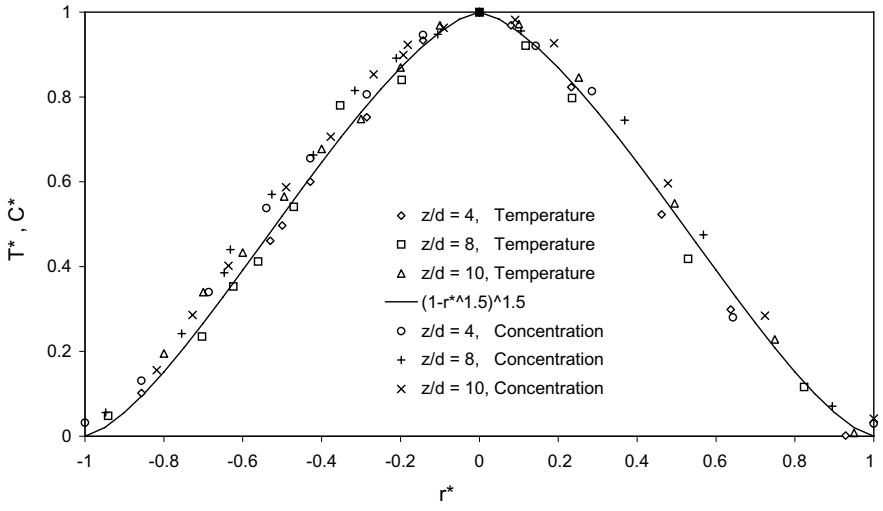

Fig. 6. Temperature and concentration profiles based on measurements.

According to turbulent jet theory [1], the radial distribution of dimensionless temperature is analogous to that of dimensionless concentration, which means the overlap of the dimensionless concentration and the temperature profiles. This analogy is validated in our experimental study, as shown in Fig. 6. It may be reasonable to assume that, in a spray jet, the radial distribution of the dimensionless temperature is still the same as that of the dimensionless concentration in a spray jet. Therefore, based on the direct measurements of oxygen concentration with a liquid nitrogen spray, both concentration and temperature radial profiles can be determined.

A recent numerical study of a liquid nitrogen spray in a dilute gas–solid suspension pipe flow suggested that the jet similarities, in the presence of evaporating liquid nitrogen droplets and dilute solid particles, is still quite similar to those of single-phase jets [11]. This result strongly supports our assumption that the dimensionless radial distribution of gas velocity in the liquid spray jet is the same as the dimensionless profile of gas velocity in the cold gas jet.

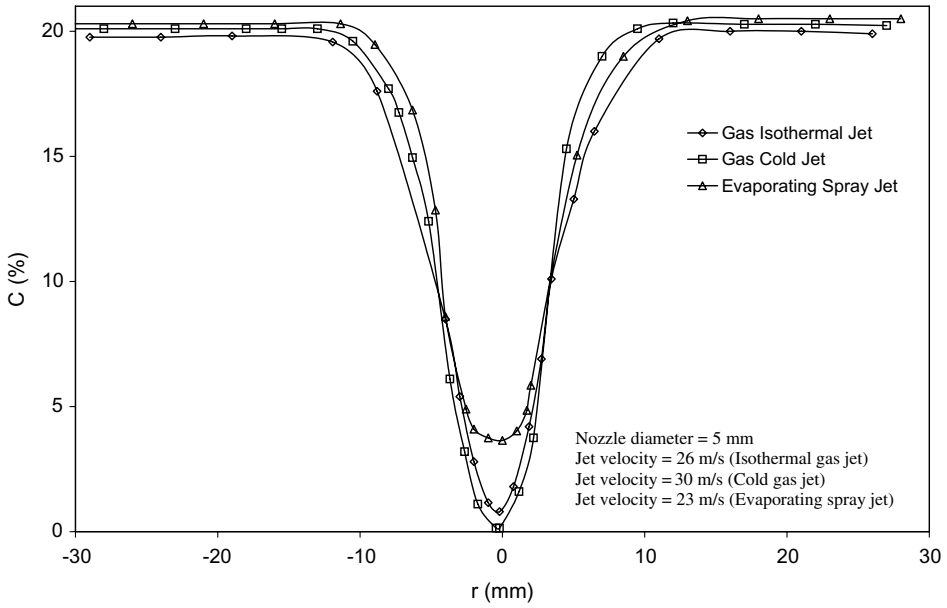

Fig. 7. Oxygen concentration profiles for different jets (at $z/d = 4$).

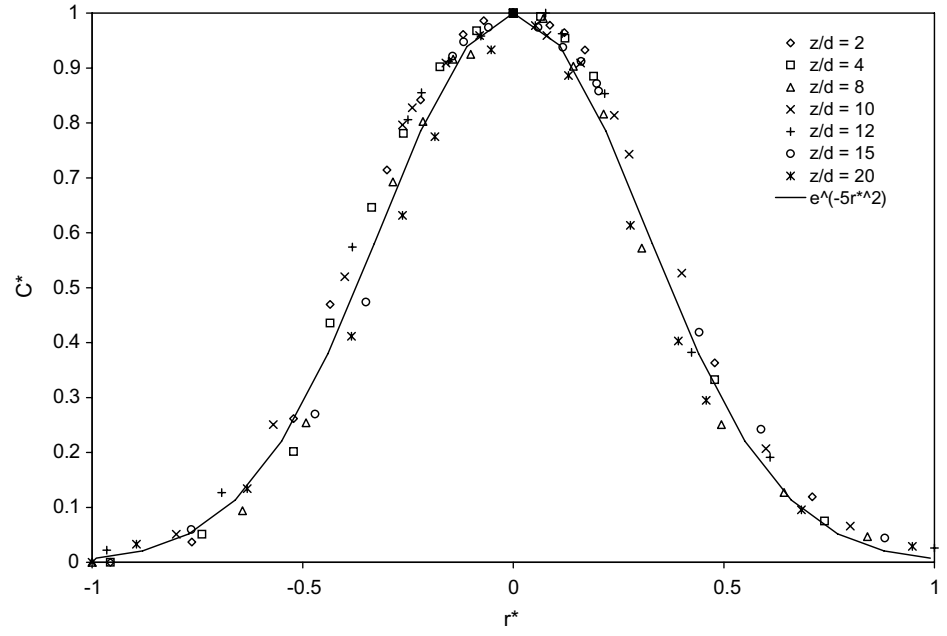

Fig. 8. Dimensionless oxygen concentration profiles in a liquid-nitrogen spray jet.

4.3. Air entrainment rate

The difference in entrainment capability of gas jets and spray jets can be qualitatively analyzed from a direct comparison of the oxygen concentration profiles at the same axial location ($z = 20$ mm), as shown in Fig. 7. At the center of jets, while the isothermal gas jet shows almost no oxygen and the cold gas jet yields a very limited amount of oxygen, the liquid nitrogen spray jet entrains a significant amount of oxygen. As the jets used in this study are of pure nitrogen, the oxygen presented inside the jets is solely due to the jet-induced entrainment. Fig. 8 shows the dimensionless profiles of oxygen concentration for a two-phase spray jet, which can be expressed by a simple semi-empirical correlation $C^* = \exp(-5r^{*2})$. The similarity curve in Fig. 8 appears somewhat skewed towards the center of the jet as compared to that of single-phase jets. This difference may be caused by the effect of radial profiles of droplet momentum and droplet evaporation rate that are not necessarily following the flow similarities. In our study, the similarity holds valid for a jet axial distance range up to z/d of 20.

4.4. Effect of evaporation on jet expansion

Fig. 9 shows the axial distribution of centerline oxygen concentration, which indicates that the oxygen concentration at the centerline of the spray jet increases much slower than those of gas jets. Fig. 10 shows the corresponding jet boundary that is determined based on oxygen concentration profiles. The results suggest that the isothermal gas jet has the least boundary expansion while the spray jet

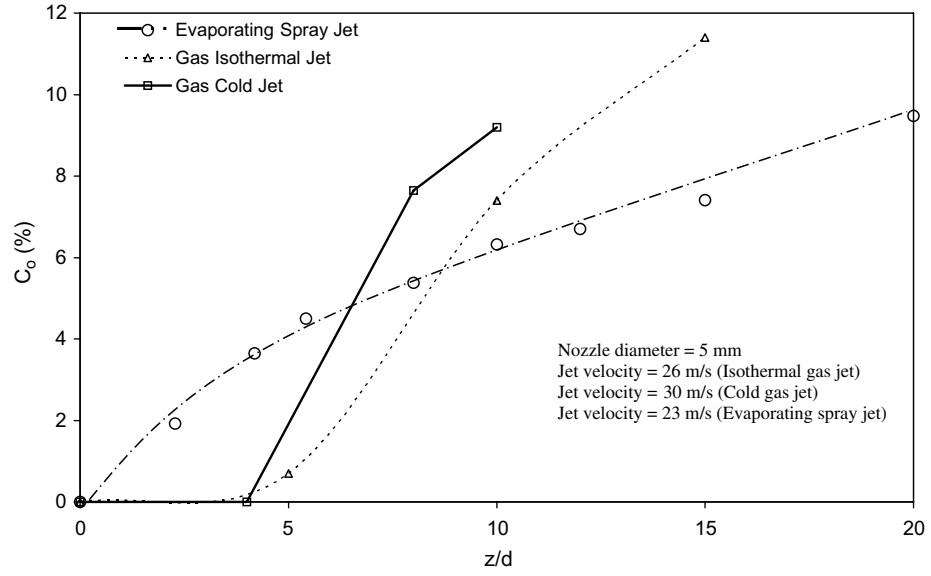

Fig. 9. Axial distribution of centerline oxygen concentration.

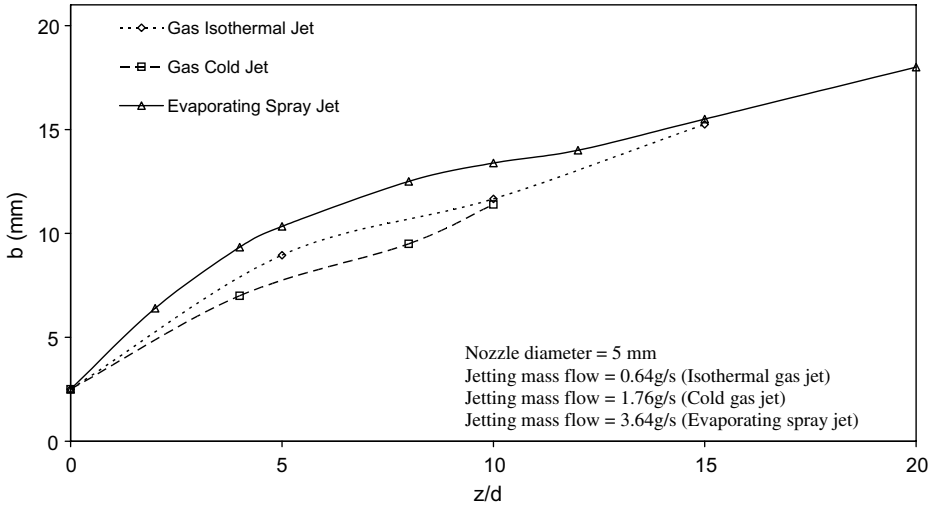

Fig. 10. Comparisons of jet boundary expansions between gas jets and spray jets.

has the maximum jet boundary expansion, especially in the initial stage of jetting where the most evaporation occurs.

4.5. Entrainment velocity

The comparison of gas centerline velocity of a spray jet and the theoretical curve of a gas jet at the same injection velocity is shown in Fig. 11. The quick decay of the centerline velocity in the initial part of the gas jet shows that the jet momentum is not able to maintain the velocity for a longer distance after exiting from the nozzle. For the spray jet, however, the decrease in the centerline gas velocity is slower. This slower decay is due to the greater inertia of droplets as well as due to the vapor generation from droplet evaporation that not only helps to sustain the gas phase velocity but also expand the jet boundary. The air entrainment velocities of gas jet and spray jet at the same jet velocity are found to be comparable, as shown in Fig. 12. However, due to the different injecting momenta between the two jets at the same jetting velocity, a more meaningful comparison should be based on the entrainment per unit injecting momentum, Due to the much higher density of droplets than the air density, entrainment per unit injecting momentum in the spray jets is at least one order of magni-

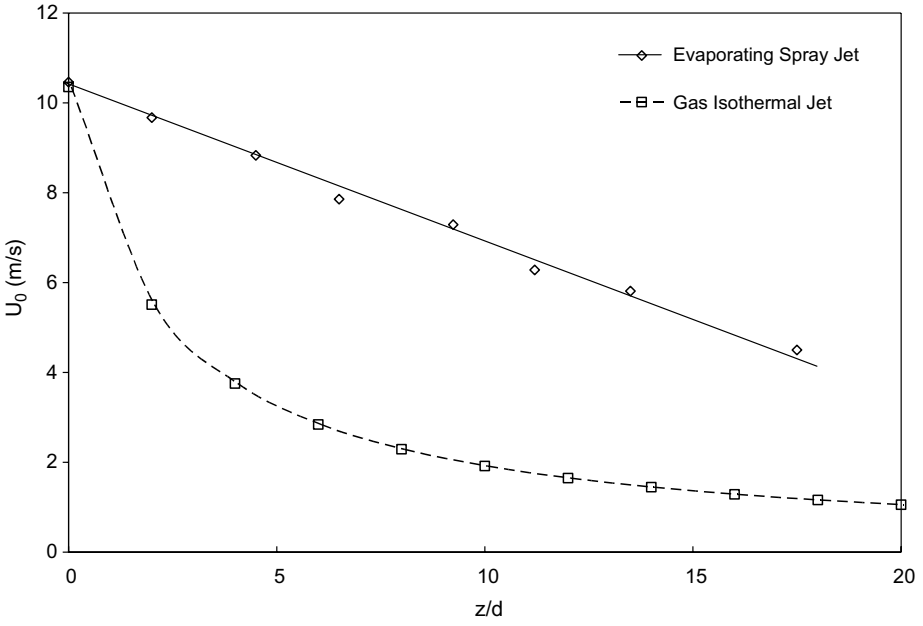

Fig. 11. Comparison of centerline velocity between gas jets and spray jets.

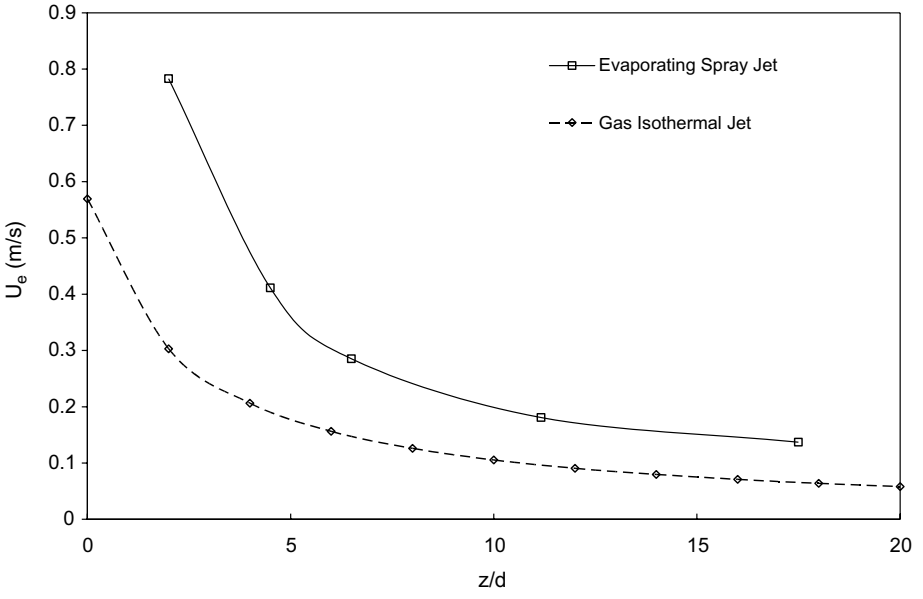

Fig. 12. Comparison of entrainment velocity between gas jets and spray jets.

tude less than that in gas jets, as shown in Fig. 13, which indicates that the rapidly evaporating spray jets have less capabilities of air entrainment than the gas jets at the same jet velocity.

4.6. Evaporation rate of spray jet

One of the objectives of this study is to estimate the evaporation rate. This is achieved by checking the energy balance at any segment of the spray jet, as expressed by Eq. (6). The axial distribution of the evaporating rate is shown in Fig. 14. A higher evaporation rate in the initial region of the spray jet is due to the higher air entrainment that brings in more thermal energy for the droplet evaporation. For the case in our study, as much as 80% of the injected liquid is evaporated within the range of *z/d* of 6. However, due to the non-uniform droplet size distribution and non-uniform jetting velocity distribution, some liquid nitrogen droplets are found to travel much further along the jet. On the average, a spray penetration length (or evaporation length) can be defined in a way that the integrated evaporation rate over that length equals the injected liquid mass flow rate, as shown in Eq. (9).

In summary, this study provides a basic methodology for the analysis on the parametric effect of spray vaporization on the gas entrainment. However, due to the simplifications we have introduced in our model, some effects have been excluded, such as effects of droplet size distribution,

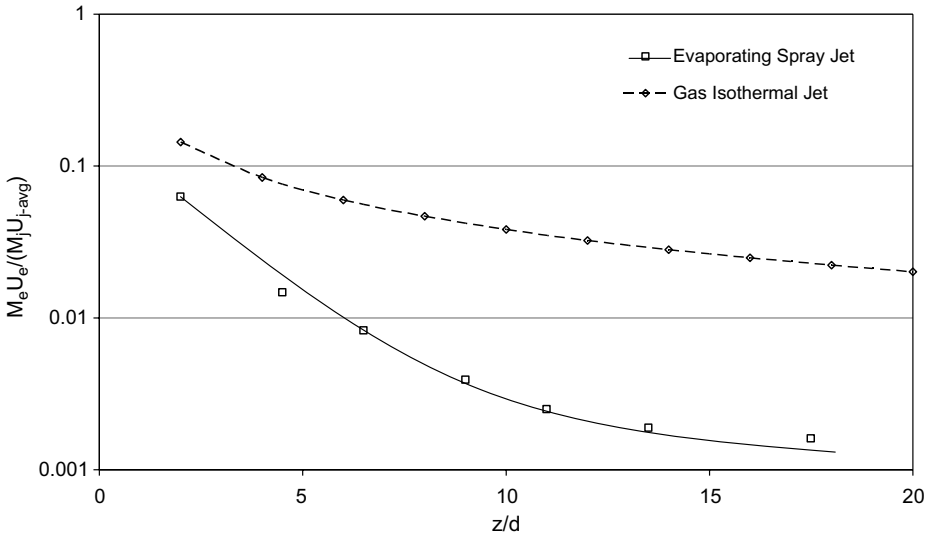

Fig. 13. Comparisons of entrained momentum between gas jets and spray jets.

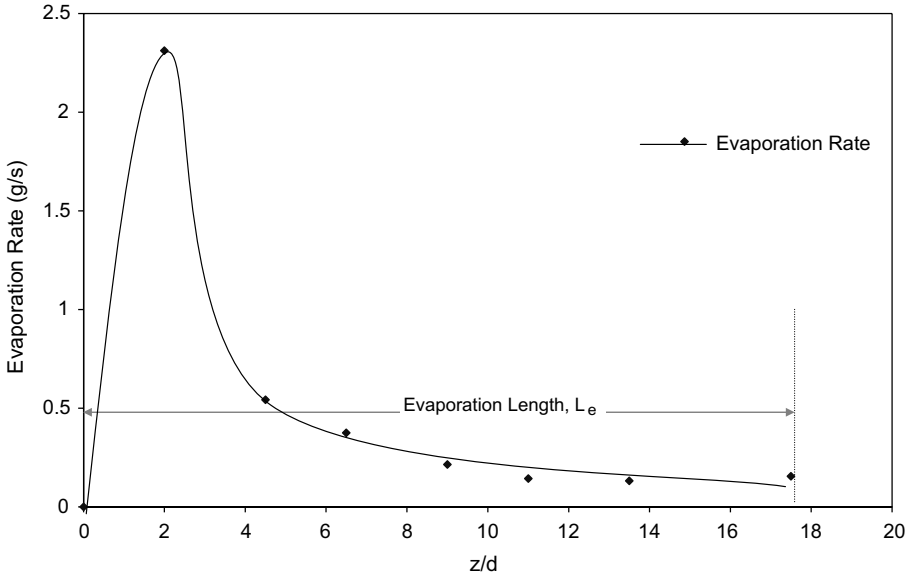

Fig. 14. Axial distribution of evaporation rate in a liquid-nitrogen spray jet.

radial distribution of droplet phases, different atomizer design, possible solidification of droplets, finite rates of heat and mass transfer, as well as local turbulence intensity and turbulence modulation by evaporating sprays. Further investigations on these effects may be desired.

5. Conclusions

A direct measurement technique of gas entrainment in an evaporating jet has been developed. A parametric model has been developed to provide the theoretical basis of data analysis for the gas entrainment. The air entrainment characteristics of the liquid nitrogen spray jet injected into the stagnant room air is found to be quite different from those of the nitrogen gas jets at the same jet velocity from the same nozzle. The measurements of gas concentration distributions in the liquid nitrogen spray jets suggest the existence of jet similarity within most of the spray jet region. The measurements further shows that the concentration-based jet boundary is wider for the spray jets than that for the gas jets whereas the entrainment per unit injecting momentum in spray jet is much less than those in the gas jets. In addition, distributions of gas velocity on the centerline and evaporation rate are also obtained.

Acknowledgements

The authors are indebted to ExxonMobil R&D Engineering Co. for their partial financial support to this project. The donors of the Petroleum Research Fund, administered by the American Chemical Society, are acknowledged for the partial support of this research under the grant of ACSPRF# 42759-AC9.

References

[1] G.N. Abramovich, The Theory of Turbulent Jets (English translation), MIT Press, Cambridge, MA, 1963.
[2] L.A. Davoust, J.L. Hammoumi, M. El, Air entrainment by a plunging jet: the dynamical roughness concept and its estimation by a light absorption technique, Int. J. Multiphase Flow 28 (2002) 1541–1564.
[3] J.R. Fincke, D.M. Crawford, S.C. Snyder, W.D. Swank, D.C. Haggard, R.L. Williamson, Entrainment in high-velocity, high-temperature plasma jets, part I: experimental results, Int. J. Heat and Mass Transfer 46 (2003) 4201–4213.
[4] R.L. Williamson, J.R. Fincke, D.M. Crawford, S.C. Snyder, W.D. Swank, D.C. Haggard, Entrainment in high-velocity, high-temperature plasma jets, part II: computational results and comparison to experiment, Int. J. Heat and Mass Transfer 46 (2003) 4215–4228.
[5] T.W. Park, V.R. Katta, S.K. Aggarwal, On the dynamics of a two-phase nonevaporating swirling jet, Int. J. Multiphase Flow 24 (1998) 295–317.
[6] S. Ghosh, J.C. Hunt, Spray jets in a cross-flow, J. Fluid Mech. 365 (1998) 109–136.
[7] D. Han, M.G. Mungal, Direct measurement of entrainment in reacting/nonreacting turbulent jets, Combust. Flame 124 (2001) 370–386.
[8] W.C. Yang, D.L. Keairns, Solid entrainment rate into gas and gas–solid two phase jets in a fluidized bed, Powder Technol. 33 (1982) 89–94.
[9] M. Filla, L. Massimilla, S. Vaccaro, Gas jets in fluidized beds: the influence of particle size, shape and density on gas and solid entrainment, Int. J. Multiphase Flow 9 (1983) 259–267.
[10] S.H. Park, H.D. Shin, Measurement of entrainment characteristics of swirling jets, Int. J. Heat and Mass Transfer 36 (1993) 4009–4018.
[11] X. Wang, C. Zhu, R. Ahluwalia, Numerical simulation of evaporating spray jets in concurrent gas–solid pipe flows, Powder Technol. 140 (2004) 56–67.
[12] X. Wang, Concurrent evaporating spray jet in dilute gas–solid pipe flows, Ph.D. thesis, New Jersey Institute of Technology, NJ, 2002.
[13] X. Wang, C. Zhu, Concentric evaporating spray jets in dilute gas–solids pipe flows, Powder Technol. 129 (2003) 59–71.